

A Pyrolysis Mechanism for Ammonia

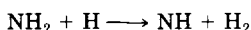
D. F. DAVIDSON, K. KOHSE-HÖINGHAUS*, A. Y. CHANG,
and R. K. HANSON

*High Temperature Gasdynamics Laboratory, Department of Mechanical Engineering,
Stanford University, Stanford, California 94305*

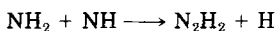
Abstract

The mechanism of NH_3 pyrolysis was investigated over a wide range of conditions behind reflected shock waves. Quantitative time-history measurements of the species NH and NH_2 were made using narrow-linewidth laser absorption. These records were used to establish an improved model mechanism for ammonia pyrolysis. The risetime and peak concentrations of NH and NH_2 in this experimental database have also been summarized graphically.

Rate coefficients for several reactions which influence the NH and NH_2 profiles were fitted in the temperature range 2200 K to 2800 K. The reaction and the corresponding best fit rate coefficients are as follows:



with a rate coefficient of $4.0 \times 10^{13} \exp(-3650/RT) \text{ cm}^3 \text{ mol}^{-1} \text{ s}^{-1}$,

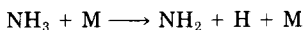


with a rate coefficient of $1.5 \times 10^{15} T^{-0.5} \text{ cm}^3 \text{ mol}^{-1} \text{ s}^{-1}$ and



with a rate coefficient of $5.0 \times 10^{13} \exp(-10000/RT) \text{ cm}^3 \text{ mol}^{-1} \text{ s}^{-1}$. The uncertainty in rate coefficient magnitude in each case is estimated to be $\pm 50\%$. The temperature dependences of these rate coefficients are based on previous estimates.

The experimental data from four earlier measurements of the dissociation reaction



were reanalyzed in light of recent data for the rate of $\text{NH}_3 + \text{H} \longrightarrow \text{NH}_2 + \text{H}_2$, and an improved rate coefficient of $2.2 \times 10^{16} \exp(-93470/RT) \text{ cm}^3 \text{ mol}^{-1} \text{ s}^{-1}$ in the temperature range 1740 to 3300 K was obtained. The uncertainty in the rate coefficient magnitude is estimated to be $\pm 15\%$.

Introduction

The ammonia decomposition system has been extensively studied; see references below. The two primary reactions in the ammonia decomposition system, $\text{NH}_3 + \text{M} \rightarrow \text{NH}_2 + \text{H} + \text{M}$ and $\text{NH}_3 + \text{H} \rightarrow \text{NH}_2 + \text{H}_2$, are sufficiently well characterized [1–5] that attention may now be focused on secondary reactions. For example, determinations of rate coefficients for certain of the reactions involving NH or NH_2 should now be possible using a detailed model and profile-fitting procedures.

* On leave from DFVLR, Institut für Physikalische Chemie der Verbrennung, D-7000 Stuttgart, W. Germany.

International Journal of Chemical Kinetics, Vol. 22, 513–535 (1990)

© 1990 John Wiley & Sons, Inc.

CCC 0538-8066/90/050513-23\$04.00

The verification of any kinetic mechanism is based on accurate quantitative measurements of the component species. At present, H and N ARAS (Atomic Resonance Absorption Spectrophotometry) measurements in shock tube experiments and atomic resonance fluorescence methods in flow reactors are capable of sensing ppm and sub-ppm levels in highly diluted systems [4–7]. NH can be measured quantitatively with a narrow-linewidth laser absorption diagnostic to a level of a few ppm [8,9]. The NH₂ narrow-linewidth laser absorption diagnostic, though it is less sensitive and the absorption coefficient is less accurately known, can be used to measure levels to approximately 10 ppm [10]. NH₃ has historically been measured by UV absorption or IR emission [1,3]. In addition to pyrolysis studies of NH₃, photolysis methods are presently available using a flashlamp [5,7] or an excimer laser [11]. These new photolytic approaches have extended the useful range of temperatures available for shock tube studies of N/H reactions below 2000 K. Thus, over a wide range of experimental conditions, it is now possible to quantitatively measure several of the important species and thereby evaluate a full kinetic mechanism of NH₃ decomposition.

Earlier ammonia pyrolysis measurements and mechanisms are summarized briefly below. As research in this field is extensive, only recently published representative studies are included.

Miller and Bowman [12] have recently reviewed the role of nitrogen chemistry in combustion. This article is a culmination of a series of articles by several workers which has introduced the role of N₂H_j species into the ammonia mechanism [13–16].

Cohen [17], a theoretical review of the O + NH₂ → NH₂ + OH reaction, contains a discussion of many of the reactions involved in ammonia decomposition.

Saliman, Hanson, and Kruger [18,19] is a shock tube study of NO and NH₃ kinetics. In their study, they followed the profiles of OH, NO, and H₂O with narrowline laser absorption, of NH₃ and N₂O by IR emission, and of NH₂ by visible emission. Their work, which uses a reaction set including the N₂H_j species, is a continuation of a NH₃/NO study begun by Roose [1,20] in our laboratory.

Dean, Chou, and Stern [21] have measured OH, NH, and NH₂ using laser absorption in atmospheric-pressure, rich ammonia flames. They have found that NH_i + NH_j reactions dominate the kinetics in these rich flames, and they have estimated several of the relevant rate coefficients.

Dasch and Blint [22] have examined lean to stoichiometric ammonia-oxygen-nitrogen flames by measuring laser-induced fluorescence, flame speed, and post-flame NO_x concentration. They found that the NH_i + NH_j reactions were not required in their modelling.

Dransfeld [23] performed direct studies of elementary reactions of NH₂ at 300 K using LMR or LIF techniques. Holzrichter and Wagner [3] have examined NH₃ decomposition at high temperatures in a shock tube with UV absorption.

Yumura and Asaba [4] performed a shock tube study of NH₃ decomposition using H ARAS. This was one of a series of articles on N/H chemistry [24–26].

Dove and Nip [2] identify H, NH, and NH₂ as playing significant roles in high temperature NH₃ decomposition and NH₂ as playing a significant role in the formation of N₂. They have derived relative concentration profiles of major species by time-resolved mass-spectroscopic analysis.

In the past decade several new facts relevant to the NH₃ system have emerged. First, an improved measurement of the rate coefficient for reaction (2), NH₃ + H → NH₂ + H, one of the primary reactions in NH₃ pyrolysis, was made by Michael, Sutherland, and Klemm [5]. In their measured temperature range, their rate coefficient value was five times larger than that previously accepted. As all the determinations of reaction (1), NH₃ + M → NH₂ + H + M, are dependent on reaction (2) and were made several years previously, it was necessary to correct them. Second, the heats of formation of several species, in particular NH₂, have been revised [27]. Finally, the role of N₂H_j species in the kinetic mechanisms has become widely accepted. These three facts, as well as a general improvement in knowledge of N/H reaction rate coefficients, have made this a suitable time to reexamine the ammonia pyrolysis mechanism.

Experimental Technique

The measurement of the NH and NH₂ concentration profiles have been performed in a high purity stock tube using narrow-linewidth laser absorption diagnostics. The experimental apparatus, which has been fully detailed in another article [10] is only briefly described here.

The shock tube driven section was stainless steel, 6.1 m long, 14.3 cm in diameter. The system was bakeable to 80°C and was turbo-pumped. The ultimate pressure and the combined leak and outgassing rate were 9×10^{-7} torr and 1.2×10^{-6} torr/min, respectively. The gases in these experiments were used directly from Liquid Carbonic cylinders. The NH₃ was >99.99% pure, while the bulk carrier gas, argon, was >99.999% pure. A passivation scheme was used in the shock tube to ensure that the mol fraction of NH₃ was then established. The shock tube was passivated with the test mixture for 5 min and then pumped for 5 min prior to refilling the tube for the shock. Infrared emission measurements at 2–3.4 μm were also used to verify the initial NH₃ concentration within ±5%.

The diagnostic beam path was either 0.95 or 2.1 cm from the endwall of the shock tube. This resulted in typical incident shock-heating times of 40 to 80 μsec (laboratory time). The temperature range and pressure in the incident shock region were 1000 to 1500 K and approximately 0.1 atm. This brief preliminary heating does not significantly affect the modelling chemistry.

Shock velocities were determined using a series of four thin films. Reflected pressure and temperatures were calculated from these velocities using a frozen chemistry, 1-dimensional shock code. The long-time temperature behavior was confirmed using the laser-scanning temperature monitor described in Chang [28] and the long-time pressure behavior was confirmed by using a piezo-electric transducer. Over the approximately 1 ms of reflected shock test time, both the pressure and temperature were found to vary no more than the experimental uncertainty of 1.5%.

The narrow-linewidth absorption laser diagnostic utilized a Spectra-Physics model 380 ring dye laser pumped either by a Spectra-Physics model 171 or 164 argon ion laser. The ring dye laser was run with Rhodamine 590 in the case of NH_2 or DCM in the case of NH. The NH_2 was detected by absorption at 597.375 nm (vac), using the $A^2A_1 \leftarrow X^2B_1(090 \leftarrow 000) \Sigma^P Q_{1,N}(7)$ doublet [10]. For NH, output of the ring dye laser was extracavity doubled with a LiIO_3 crystal. The NH was detected by absorption using either the $A^3\Pi_i \leftarrow X^3\Sigma(0,0)Q_1$ band head at 336.100 nm or the single $Q_2(9)$ line at 336.060 nm [8].

The absorption coefficient for NH (used in the Beer-Lambert law conversion of the experimental absorption data to mol fraction) is directly related to the radiative lifetime of the upper state of the absorption transition [8]. The coefficient used here is based on a measurement of 420 ns for the lifetime of the $v = 0$ level of NH ($A^3\Pi_i$) by Garland and Crosley [29]. This has been stated to be accurate within 2%. This uncertainty is combined with the experimental uncertainty in locating the laser at the absorption peak ($\pm 0.02 \text{ cm}^{-1}$ on a 0.2 cm^{-1} FWHM line for NH_2 and $\pm 0.04 \text{ cm}^{-1}$ on a 0.30 cm^{-1} FWHM line for NH) and the uncertainty in determining the mol fraction which accrue from finite the signal-to-noise ratios, the errors in gas mixtures, and the shock tube temperature determination. The overall uncertainty in mol fraction is $\pm 10\%$.

In the case of NH_2 there is at present no final consensus on the oscillator strength for the $A^2A_1 \leftarrow X^2B_1(900 \leftarrow 000) \Sigma^P Q_{1,N}(7)$ transition. This transition, a pair of overlapping lines, has also been described by a different notation [42]. Recent work in our laboratory by Kohse-Höinghaus [10] gives an absorption coefficient based on both kinetic and photolysis techniques. The claimed accuracy is $\pm 30\%$. For the present work the pyrolysis NH_2 profiles are self calibrating, as the early time NH_2 behavior is well described by the two known reactions: (7), $\text{NH}_3 + \text{M} \rightarrow \text{NH}_2 + \text{H} + \text{M}$, and (15), $\text{NH}_3 + \text{H} \rightarrow \text{NH}_2 + \text{H}_2$. Fitting the early time slope for each shock datum in the current study however, gives absorption coefficients consistent with the upper limits of the absorption coefficients given by Kohse-Höinghaus.

Synopsis of the Experimental Database

The pyrolysis experiments were conducted in the temperature range 2000 to 3200 K, in the pressure range 1.1 to 0.8 atm, and in the concentration range 0.1 to 1.0% NH_3 . A small group of NH_2 absorption experiments was conducted at 0.4 to 0.5 atm. Examples of the data and the good fits obtained with the final mechanism are shown in Figures 1 to 4.

To allow tests and comparisons of future revised mechanisms, the pyrolysis NH and NH_2 peaks were characterized in two ways. The experimentally measured values of the peak concentration for both NH and NH_2 are shown in Figure 5. The time interval between the arrival of the reflected shock front and the occurrence of the peak mol fraction (i.e., the "time-to-peak") is shown in Figure 6. The reflected shock pressures for these experiments are best described (independent of NH_3 concentration) as $P = -3.25 \times 10^6 T^{-2} + 4.26 \times 10^3 T^{-1} - 0.236$ [atm] ($\pm 3\%$).

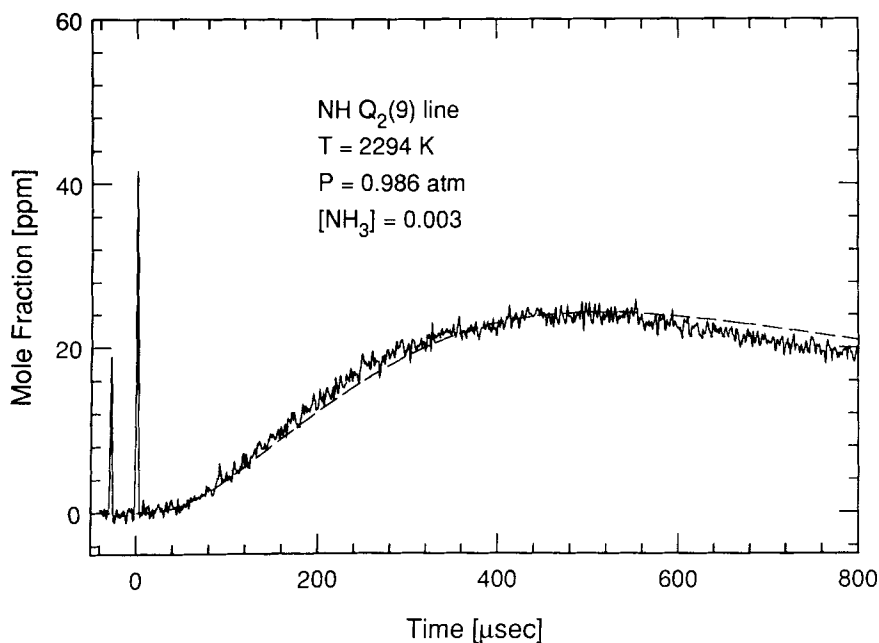


Figure 1. NH ($Q_2(9)$ line) absorption data and kinetic model. Reflected shock conditions are $T = 2294$ K, $P = 0.986$ atm, and $[\text{NH}_3] = 0.003$. The two peaks at time 0 and -30 μs are the result of shock front induced beam steering.

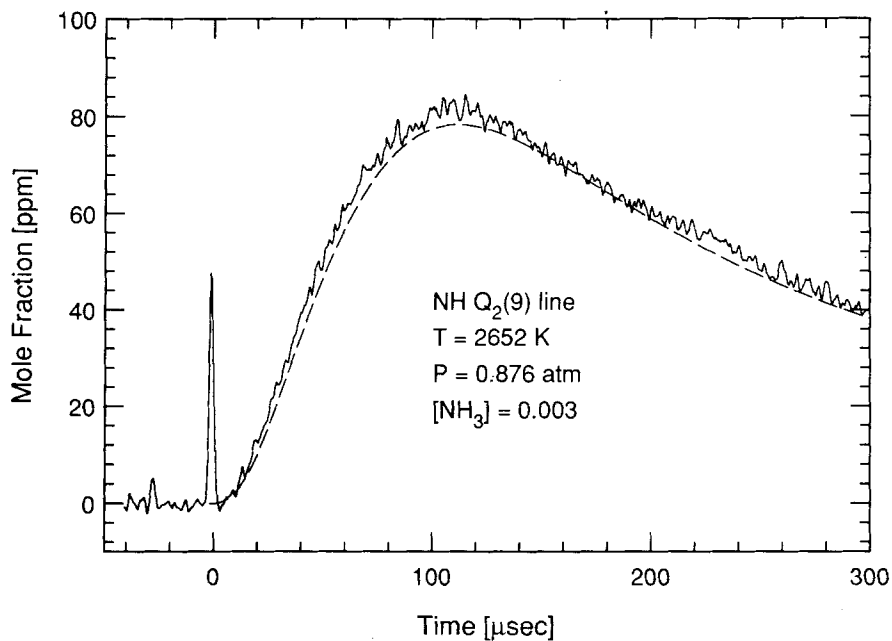


Figure 2. NH ($Q_2(9)$ line) absorption data and kinetic model. Reflected shock conditions are $T = 2652$ K, $P = 0.876$ atm, and $[\text{NH}_3] = 0.003$.

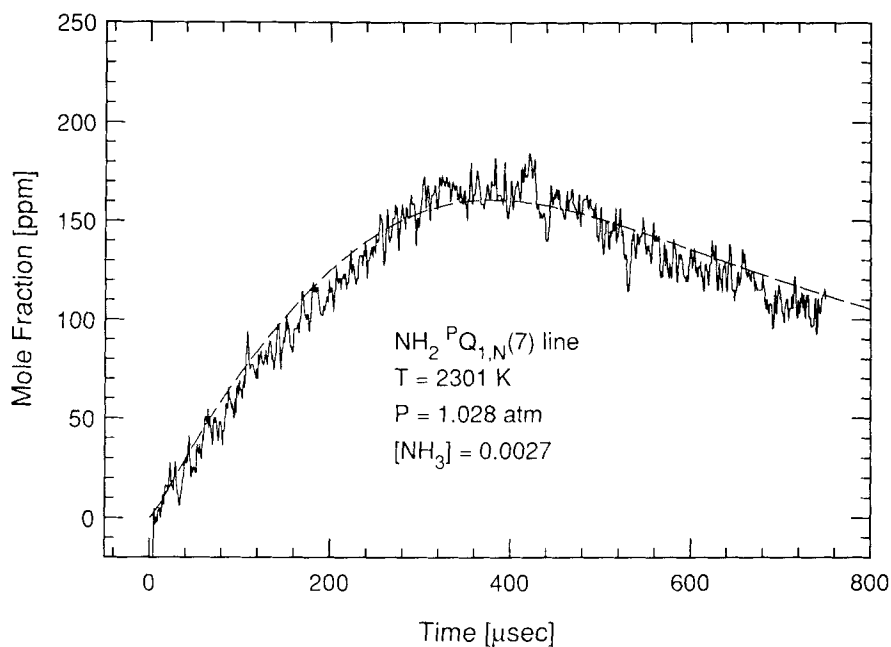


Figure 3. NH_2 (${}^P Q_{1,N}(7)$ line) absorption data and kinetic model. Reflected shock conditions are $T = 2301$ K, $P = 1.028$ atm, and $[\text{NH}_3] = 0.0027$.

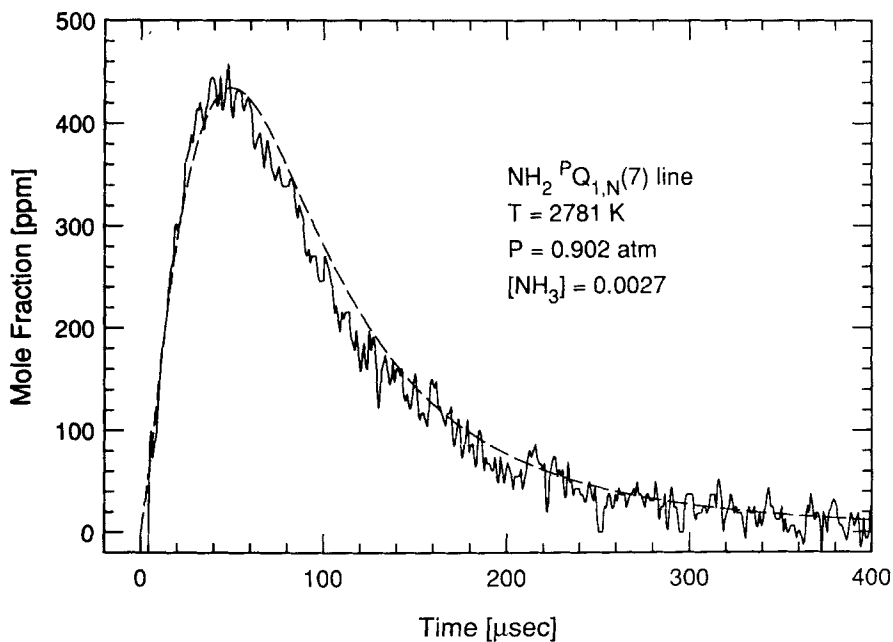


Figure 4. NH_2 (${}^P Q_{1,N}(7)$ line) absorption data and kinetic model. Reflected shock conditions are $T = 2781$ K, $P = 0.902$ atm, and $[\text{NH}_3] = 0.0027$.

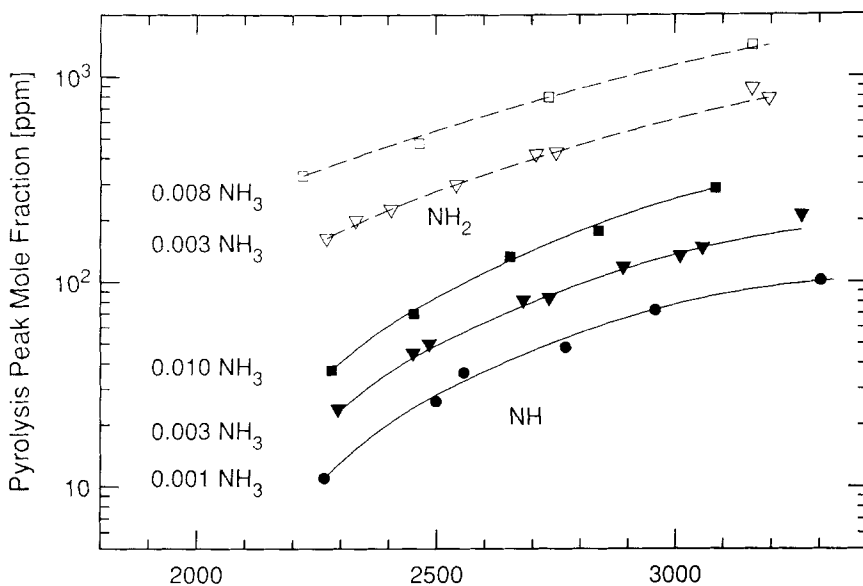


Figure 5. Peak mol fractions of NH and NH₂ occurring during the pyrolysis of NH₃. Best fit to our database is shown as lines. Solid lines and symbols are the NH peak values, and dashed lines and hollow symbols are the NH₂ values. Circles: 0.001 [NH₃]; triangles: 0.003 [NH₃]; and squares: 0.008/0.01 [NH₃]. The reflected shock pressures for the experiments in Figures 5 and 6 (independent of NH₃ concentrations) are given by $P[\text{atm}] = -3.25 \times 10^6 T^{-2} + 4.26 \times 10^3 T^{-1} - 0.236$ ($\pm 3\%$).

The NH₂ time-to-peak are determined mainly by reaction (1), $\text{NH}_3 + \text{M} \rightarrow \text{NH}_2 + \text{H} + \text{M}$. Thus the time-to-peak values (at any fixed temperature and similar pressures) for all measured NH₃ concentrations collapse to a single point. The NH₂ times-to-peak for the 0.3% NH₃, 0.4 to 0.5 atm cases (done at half the pressure of the nominal 1 atm experiments) are twice as long.

The Kinetic Model

The complete mechanism is shown in Table I. A discussion of individual reactions included in (and excluded from) this mechanism is given in the Appendix. The mechanism is derived from the recent article by Miller and Bowman [12] and includes their relevant N/H reactions.

Recent measurements of some NH reactions have provided more confidence in the secondary and tertiary reaction sequence of this mechanism. These recent measurements include the work of Mertens [9] on reactions (4), $\text{NH} + \text{M} \rightarrow \text{N} + \text{H} + \text{M}$, and (7), $\text{NH} + \text{NH} \rightarrow \text{N}_2 + \text{H} + \text{H}$, and the work of Davidson [30] on reaction (5), $\text{N} + \text{H}_2 \rightarrow \text{H} + \text{NH}$. Another recent work utilized is the room temperature study of reaction (1), $\text{NH} + \text{NH}_2 \rightarrow \text{products}$, by Dransfeld [23].

Shown in Figure 7 are the kinetic modelling predictions for all the species which are expected to be present in a typical NH₃ pyrolysis reflected-shock experiment at the conditions of 2500 K, 1 atm, 0.3% NH₃. The CHEMKIN program has been used for the computation (constant enthalpy,

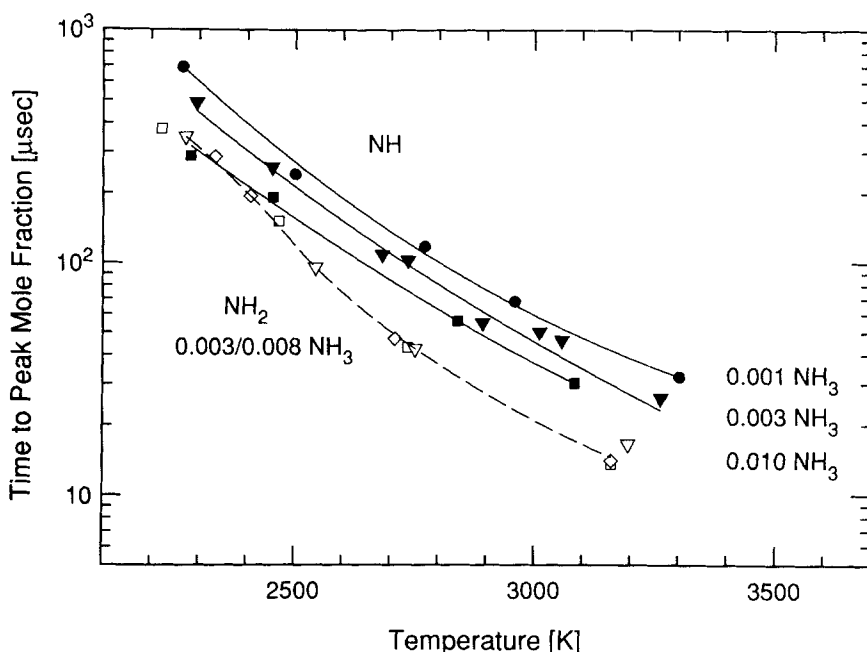


Figure 6. Time-to-peak mol fraction of NH and NH₂ during pyrolysis in various NH₃ concentrations. Solid lines and symbols are the NH peak values and the dashed lines and hollow symbols are the NH₂ values. Circles: 0.001 [NH₃]; triangles: 0.003 [NH₃]; and squares: 0.008/0.001 [NH₃]. Times indicated for the 0.5 atm experiments (shown here as hollow diamonds) are the experimental values divided by two.

constant pressure) [31]. The equilibrium products H₂ and N₂ exceed the reactant concentrations after 400 μ sec. The important intermediaries NH₂, H, NH, and N rapidly form in that sequence. NH₂ disappears rapidly, while NH disappears slowly. The rapidly-turned-over species, N₂H₂ and NNH, never reach 1 ppm but are the major route for the formation of N₂. The heavier products N₂H₃ and N₂H₄ form in insignificant amounts and do not affect the modelled profiles of the measured species.

Contribution and Sensitivity Analysis

The contribution factors for the species NH₂ and NH are shown in Figures 8 and 9. The contribution factor is the net production (or loss) rate of a species due to a particular reaction.

The two major loss reactions for NH₃ are also the primary production paths for NH₂. It can be assumed that the alternate route of reaction (1a), NH₃ + M \rightarrow NH + H₂, is insignificant compared to the primary route [1,3]. The primary loss reactions for NH₂ result from collisions with H, NH, and NH₂.

The primary production of NH is from reaction (9), NH₂ + H \rightarrow NH + H₂, and from reaction (12), NH₂ + NH₂ \rightarrow NH + NH₃. The loss routes for NH are reactions with H, NH, and NH₂. These loss rates are effectively gas kinetic with no strong temperature dependence. Reactions (9) and (11)

TABLE I. Ammonia pyrolysis mechanism.

#	REACTIONS	ΔH_{298}°	A	b	E_A	Ref.
1	$\text{NH}_3 + \text{M} = \text{NH}_2 + \text{H} + \text{M}$	108.52	2.20E16	0.0	93468.	*
2	$\text{NH}_3 + \text{H} = \text{NH}_2 + \text{H}_2$	4.45	6.36E05	2.39	10171.	5
3	$\text{H}_2 + \text{M} = \text{H} + \text{H} + \text{M}$	104.14	2.19E14	0.0	95970.	38
4	$\text{NH} + \text{M} = \text{N} + \text{H} + \text{M}$	79.80	2.65E14	0.0	75500.	9
5	$\text{NH} + \text{H} = \text{H}_2 + \text{N}$	-24.34	3.60E13	0.0	325.	30
6	$\text{NH} + \text{N} = \text{N}_2 + \text{H}$	-146.00	3.00E13	0.0	0.	12
7	$\text{NH} + \text{NH} = \text{N}_2 + \text{H} + \text{H}$	-66.20	5.10E13	0.0	0.	9
8	$\text{NH}_2 + \text{M} = \text{NH} + \text{H} + \text{M}$	91.76	3.16E23	-2.0	91400.	34
9	$\text{NH}_2 + \text{H} = \text{NH} + \text{H}_2$	-12.38	4.00E13	0.0	3650.	*
10	$\text{NH}_2 + \text{N} = \text{N}_2 + \text{H} + \text{H}$	-54.24	7.20E13	0.0	0.	12
11	$\text{NH}_2 + \text{NH} = \text{N}_2\text{H}_2 + \text{H}$	-27.68	1.50E15	-0.5	0.	*
12	$\text{NH}_2 + \text{NH}_2 = \text{NH}_3 + \text{NH}$	-16.76	5.00E13	0.0	10000.	*
13	$\text{NH}_2 + \text{NH}_2 = \text{N}_2\text{H}_2 + \text{H}_2$	-40.06	5.00E11	0.0	0.	12
14	$\text{NNH} + \text{M} = \text{N}_2 + \text{H} + \text{M}$	-6.47	2.00E14	0.0	20000.	12
15	$\text{NNH} + \text{H} = \text{N}_2 + \text{H}_2$	-110.61	4.00E13	0.0	3000.	34
16	$\text{NNH} + \text{NH} = \text{N}_2 + \text{NH}_2$	-98.23	5.00E13	0.0	0.	12
17	$\text{NNH} + \text{NH}_2 = \text{N}_2 + \text{NH}_3$	-114.99	5.00E13	0.0	0.	12
18	$\text{N}_2\text{H}_2 + \text{M} = \text{NNH} + \text{H} + \text{M}$	59.71	5.00E16	0.0	50000.	12
19	$\text{N}_2\text{H}_2 + \text{H} = \text{NNH} + \text{H}_2$	-44.43	5.00E13	0.0	1000.	12
20	$\text{N}_2\text{H}_2 + \text{NH} = \text{NNH} + \text{NH}_2$	-32.05	1.00E13	0.0	1000.	12
21	$\text{N}_2\text{H}_2 + \text{NH}_2 = \text{NNH} + \text{NH}_3$	-48.81	1.00E13	0.0	1000.	12

The rate coefficients are expressed as $AT^b \exp(-E_A/RT)$ [$\text{cm}^3 \text{mol}^{-1} \text{s}^{-1}$]. The heats of formation are in units of kcal/mol^{-1} . The activation energies are in units of cal mol^{-1} . * indicates that the rate coefficient is determined in this work.

have similar shaped contribution plots and experimentally it is difficult to distinguish their component contribution to the NH profile.

The sensitivity coefficient is defined as [32]

$$X_{ij}(t) = A_j / X_i^{\max} (dX_i / dA_j)(t)$$

where $X_{ij}(t)$ is the sensitivity coefficient for a change in the mol fraction of the i th species due to a small change in the temperature independent factor in the j th reaction rate coefficient A_j , and X_i^{\max} indicates the maximum value of X_i that occurred in the calculated profile.

The sensitivity plots for NH_2 and NH are shown in Figures 10 and 11. Only reactions that yield greater than 10% of the sensitivity of the largest reaction are shown. The sensitivity analysis computation has been per-

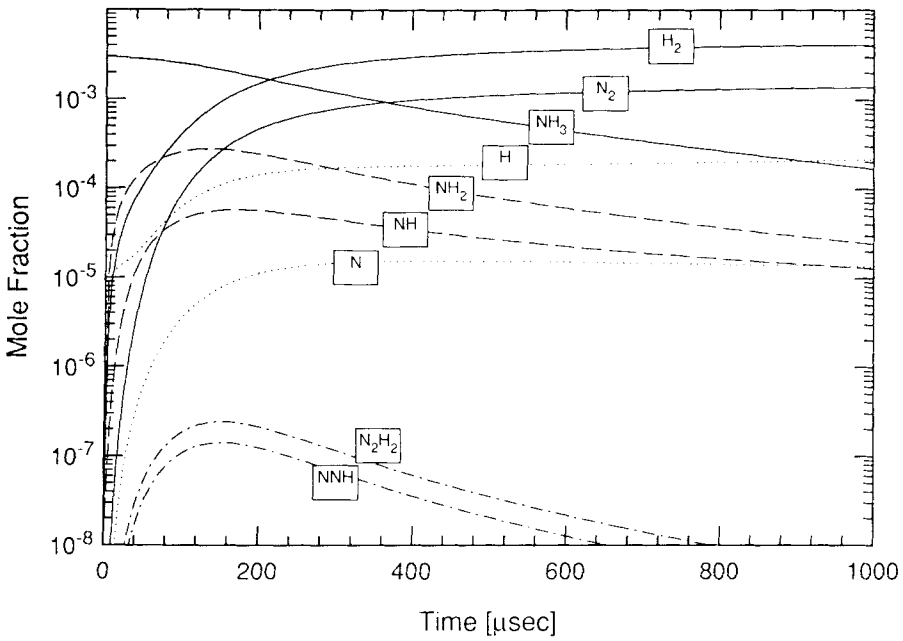


Figure 7. Mol fraction time-histories for all major species in pyrolysis kinetic model. Modelled shock conditions are $T = 2500$ K, and $P = 1.00$ atm $[NH_3] = 0.003$. N_2H_3 and N_2H_4 exist in concentrations at or below 10^{-9} .

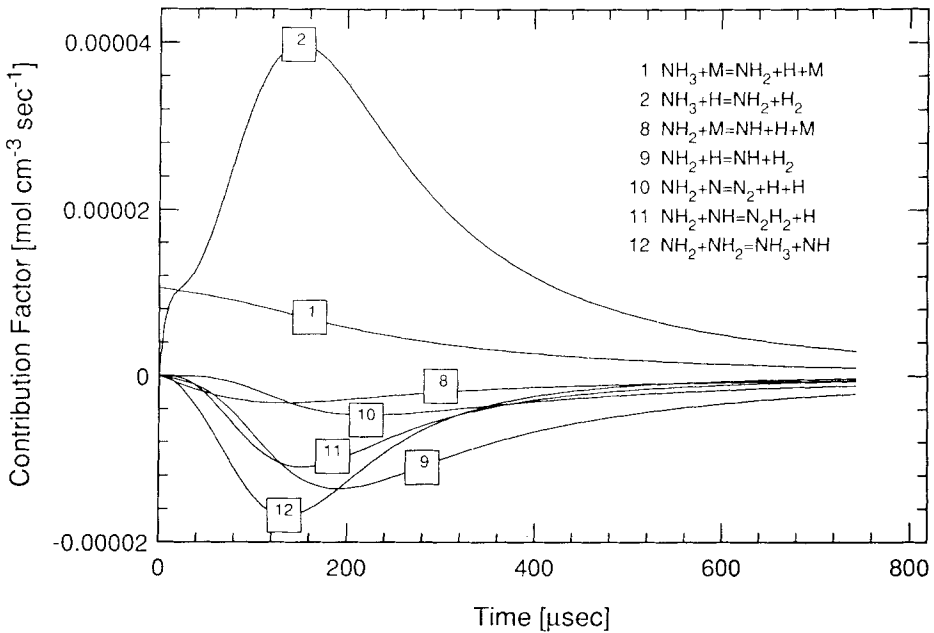


Figure 8. NH_2 reactions contributions. Only reactions whose values are 10% or more of the largest contributor are included. Model conditions are the same for Figure 7.

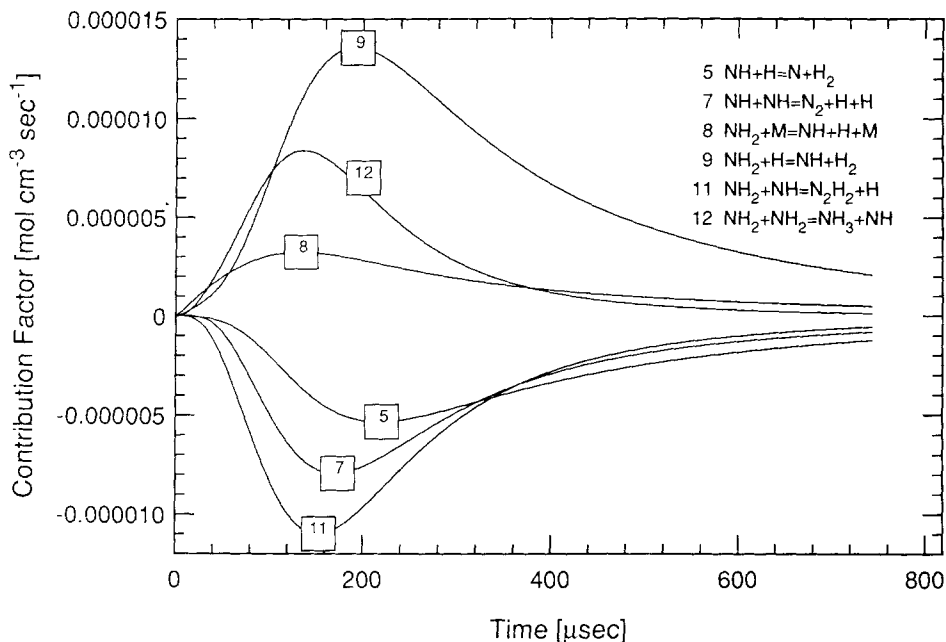


Figure 9. NH reaction contributions. Only reactions whose values are 10% or more of the largest contributor are included. Model conditions are the same for Figure 7.

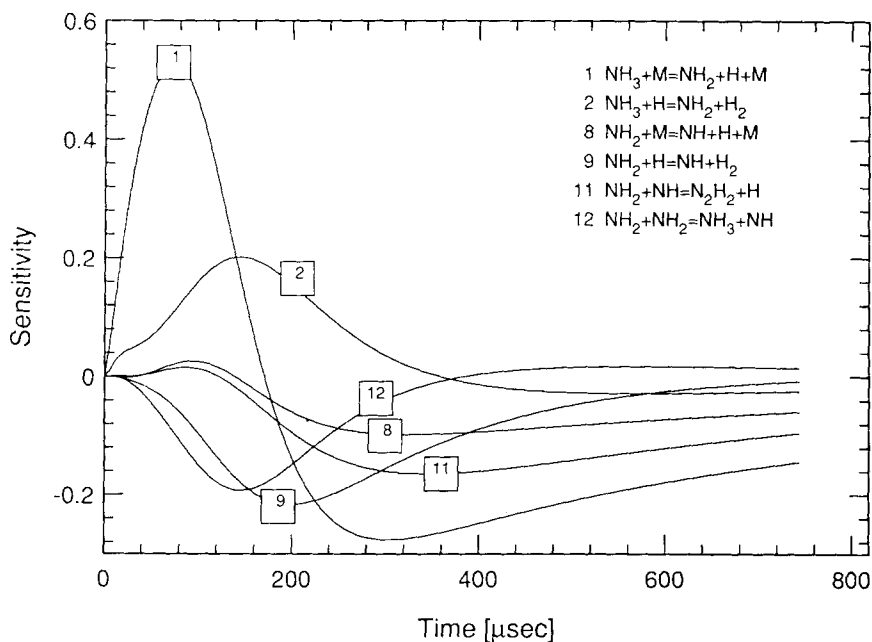


Figure 10. NH_2 sensitivity analysis. Only reactions whose sensitivity coefficient values are 10% or more of the most sensitive are included. Model conditions are the same as for Figure 7.

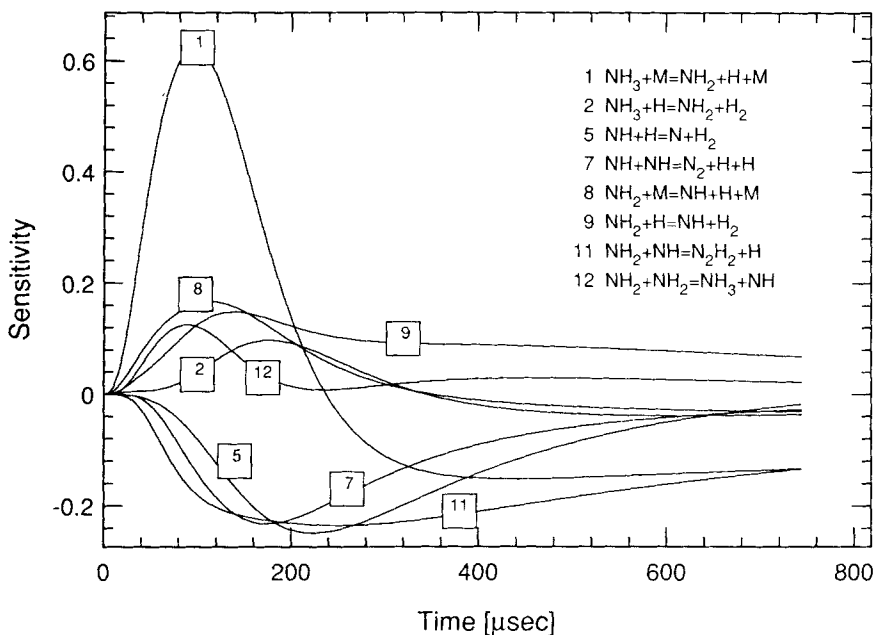


Figure 11. NH sensitivity analysis. Only reactions whose sensitivity coefficient values are 10% or more of the most sensitive are included. Model conditions are the same as for Figure 7.

formed using the SENKIN [32] program and a discussion of the mathematical definition for the sensitivity coefficient may be found there.

The NH_2 mol fraction is most sensitive to k_1 and k_2 , and somewhat less sensitive to k_9 and k_{12} . The NH mol fraction is particularly sensitive to the rate coefficient k_1 . Several other minor reactions have lower and approximately equal sensitivity at various times in the decomposition.

Of the reactions that influence the time histories of NH_2 and NH, rate coefficients for reactions (8), (9), (11), and (12) have not been measured directly at high temperatures.

Heats of Formation

Andersen [27] has recently surveyed the literature on the heats of formation of NH and NH_2 , and his recommended values are very close to the values in the Sandia Database which are used in this study [32]. The Sandia Database is similar to the JANAF data for all species except NH and NNH. $H^\circ(298)$ for NH_2 is $45.50 \text{ kcal mol}^{-1}$; $H^\circ(298)$ for NH is $85.20 \text{ kcal mol}^{-1}$. One consequence of the uncertainty in the knowledge of the heats of formation for N/H species is its effect on the uncertainty of the modelled NH profiles. Andersen gives an uncertainty of $\pm 0.5 \text{ kcal mol}^{-1}$ for $H^\circ(298)$ for NH. This gives an added $\pm 10\%$ uncertainty in k_5 , ($\text{H} + \text{NH} \rightarrow \text{N} + \text{H}_2$), one of the dominant loss mechanisms of NH, as this rate was originally measured in the reverse direction [30].

Discussion

In this section, the rate coefficients of four reactions are discussed. The new determination of the rate coefficient for reaction (1), $\text{NH}_3 + \text{M} = \text{NH}_2 + \text{H} + \text{M}$, is based on a re-analysis of four previous studies. The determination of the three rate coefficients, of reactions (9), (11), and (12), are based on a comparison of the experimentally determined NH and NH_2 profiles with that of the modelled profiles. All rate coefficients given in this article are in units of $\text{cm}^3 \text{mol}^{-1} \text{s}^{-1}$ with activation energies in cal mol^{-1} .



The low pressure limit of this reaction has been reviewed by Hanson and Salimian [34]. They give a value of the rate coefficient of $2.51 \times 10^{16} \exp(-93790/RT)$ ($\pm 35\%$) derived from work by Roose [1]. Three other primary references for this rate, Yumura and Asaba [4], Holtzrichter and Wagner [3], and Dove and Nip [2] differ in varying degrees from Roose's value. All four of these works were done before Michael, Sutherland, and Klemm's improved determination of k_2 in 1985 [5]. We have found that it is possible to reconcile these four works and achieve smaller overall uncertainty if the newer value for the rate coefficient of reaction (2), $\text{NH}_3 + \text{H} \rightarrow \text{NH}_2 + \text{H}$, is used in a reanalysis of these studies.

The method used by all four groups was to derive the rate coefficient from the early time behavior of one of NH_3 , NH_2 , or H , in dilute mixtures of NH_3 in argon (krypton in the case of Dove and Nip). The slope derived from the initial rate (of formation or of loss) can be simply corrected (to first order) to allow for the contribution of the competing reaction (2). For the three experiments measuring NH_3 or NH_2 concentrations, this correction lowers the rate coefficient, and for those of Yumura and Asaba measuring H , it increases the rate coefficient. The correction is based on values which are given in each article of the typical time used to determine the slope, the typical concentration of NH_3 , the rate coefficients employed for $\text{NH}_3 + \text{H}$, and the temperature. The rate coefficient correction is of the form

$$k_{1\text{corr}} = k_{1\text{uncorr}} / (1 \pm \Delta k_2 [\text{NH}_3] \Delta t)$$

where the plus sign is used for NH_3 and NH_2 measurements and the minus sign is used in the case of H atom measurements.

Using this procedure and the published conditions of the measurements, the rate coefficients of all four studies have been adjusted and are found to be within $\pm 15\%$ of the rate coefficient derived in Roose's work. This corrected value is $2.20 \times 10^{16} \exp(-93470/RT)$. The original and corrected values are shown in Figure 12.

Holtzrichter and Wagner [2] discuss the role of reaction (1a), $\text{NH}_3 + \text{M} = \text{NH} + \text{H}_2 + \text{M}$, but argue that it is not significant in the decomposition of NH_3 based on the early time emission of NH . Roose, based on a similar emission experiment, gives as an upper limit to this rate coefficient a value of $6.3 \times 10^{14} \exp(-93390/RT)$, at least 40X less than the dominant channel.

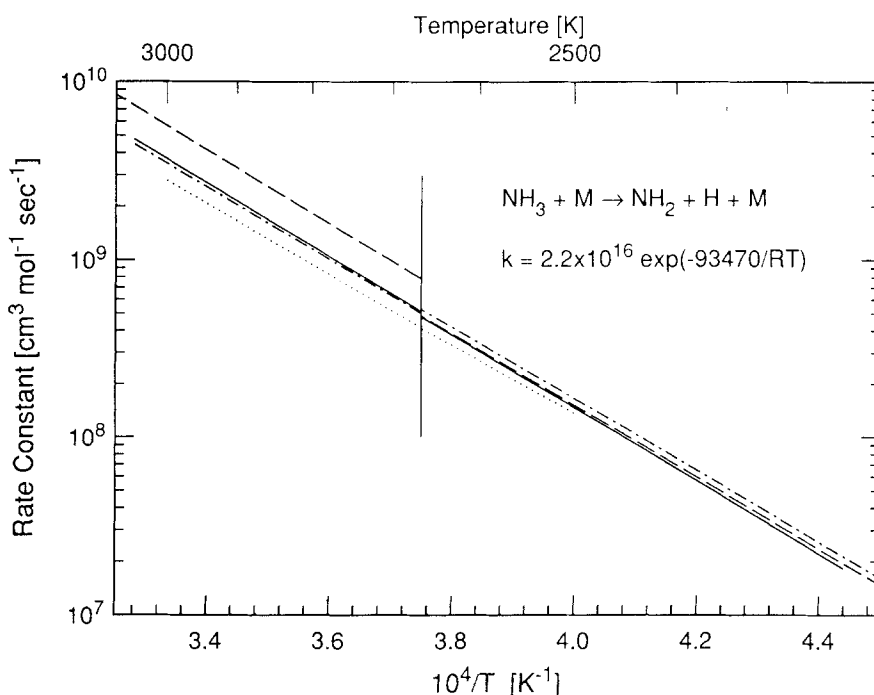
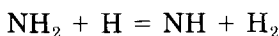


Figure 12. Arrhenius plot for reaction (1): $\text{NH}_3 + \text{M} \rightarrow \text{NH}_2 + \text{H} + \text{M}$. Solid line: Roose [1]; dotted line: Dove and Nip [2]; dashed line: Holzrichter and Wagner [3]; and dot-dashed line: Yumura and Asaba [4]. Original results shown above 2650 K, corrected values of the rate coefficient shown below 2650 K.



We have found only five published determinations of k_9 ; four from experiment and one from a theoretical estimate. These are shown in Figure 13.

Roose [1] has used NH emission in NH_3 pyrolysis at 2800 K and has obtained a value of 3.9×10^{13} . His suggested extrapolation of this rate coefficient to lower temperatures is $6.92 \times 10^{13} \exp(-3650/RT)$. Miller [12–16] have used the rate coefficient of Roose successfully for modelling of flames. As well, they have found that the use of the temperature dependence for this reaction suggested by Yumura and Asaba results in drastic changes in flame profiles and have degraded the agreement between these model predictions and experiment.

In shock tube ammonia pyrolysis experiments in the temperature range 2600 to 2800 K, Dove and Nip [2] have studied the reverse reaction and have obtained $k_{-9} = 2 \times 10^{12}$. At 2700 K this is equivalent to $k_9 = 2.88 \times 10^{13}$.

Yumura and Asaba [26] have studied reaction (9) in hydrazine shock tube experiments in the temperature range 2230 to 3460 K and give $k_9 = 4.47 \times 10^{13} \exp(-10440/RT)$. They provide additional discussion of this reaction in their NH_3 pyrolysis study [4].

Dean, Lyon, and Hardy [21] have found that a rate two times that found in Bahn [35] gave satisfactory fits to their flame data. Bahn [35] lists a theoretical estimate of this rate coefficient from the work of Mayer [36,37]. The value of Mayer is $k_9 = 5 \times 10^{11} T^{0.5} \exp(-2000/RT)$.

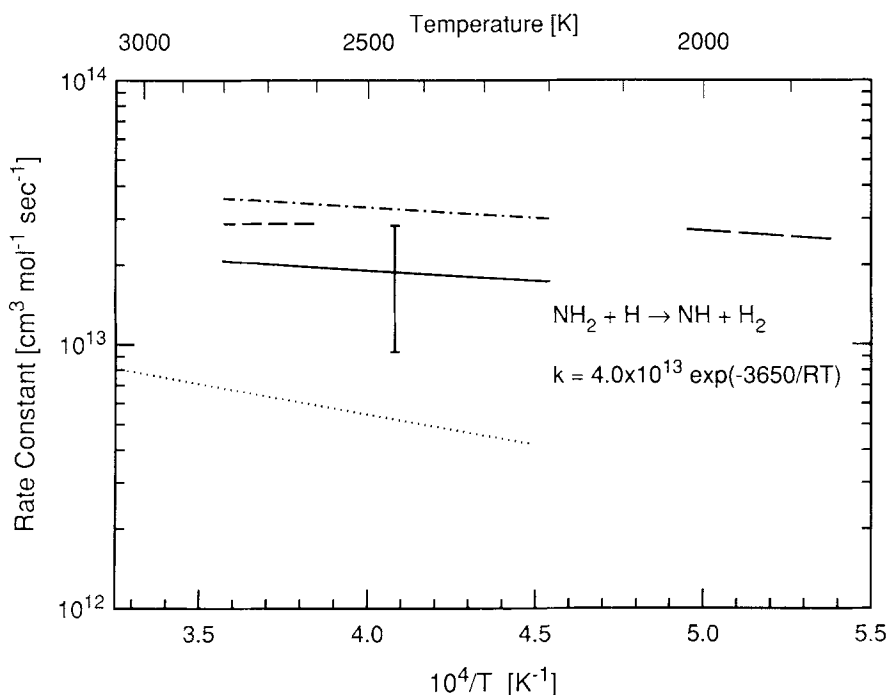
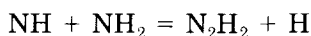


Figure 13. Arrhenius plot for reaction (9): $\text{NH}_2 + \text{H} = \text{NH} + \text{H}_2$. Solid line: present work, $\pm 50\%$ error bar; dashed line: Dove and Nip [2]; dot-dashed line: Roose [1]; dotted line: Yumura and Asaba [26]; and long-dashed line: Dean, Chou, and Stern [21].

Our determination of this rate coefficient is closely related to the selection of the rate coefficient for reaction (11): $\text{NH} + \text{NH}_2 \rightarrow \text{N}_2\text{H}_2 + \text{H}$. The shapes of their contribution factors are similar in NH_3 pyrolysis experiments and, because of this subtlety, it is necessary to fit both NH and NH_2 over a large range of conditions to place constraints on these rate coefficients. The NH_2 data has been fit to the decay region in the temperature range 2200 to 2800 K. The NH data has been fitted over both the rise and the fall.

We find the best fit is given by $k_9 = 4 \times 10^{13} \exp(-3650/RT)$ ($\pm 50\%$). Efforts to closely represent the database with values beyond $\pm 50\%$ of this rate coefficient require unrealistic values for k_{11} or k_{12} . Examples of the effect on the NH and NH_2 profiles in this model by varying this rate coefficient by $\pm 50\%$ are shown in Figure 14. The data do not allow a temperature dependence to be determined, and the activation energy of Roose is used. The activation energy of Roose is based on a two parameter fit to the estimate of Mayer. The best fit value to our database is in agreement with Dove and Nip [2] and the theoretical estimate of Mayer [36,37].



The rate coefficient for this reaction at high temperatures has previously only been estimated. Miller [14] state that this reaction can be compared to the isoelectric reactions $\text{NH} + \text{OH} \rightarrow \text{HNO} + \text{H}$ for which they give $k = 2 \times 10^{13}$, and $\text{O} + \text{NH}_2 \rightarrow \text{HNO} + \text{H}$ which they give as $k = 6.63 \times$

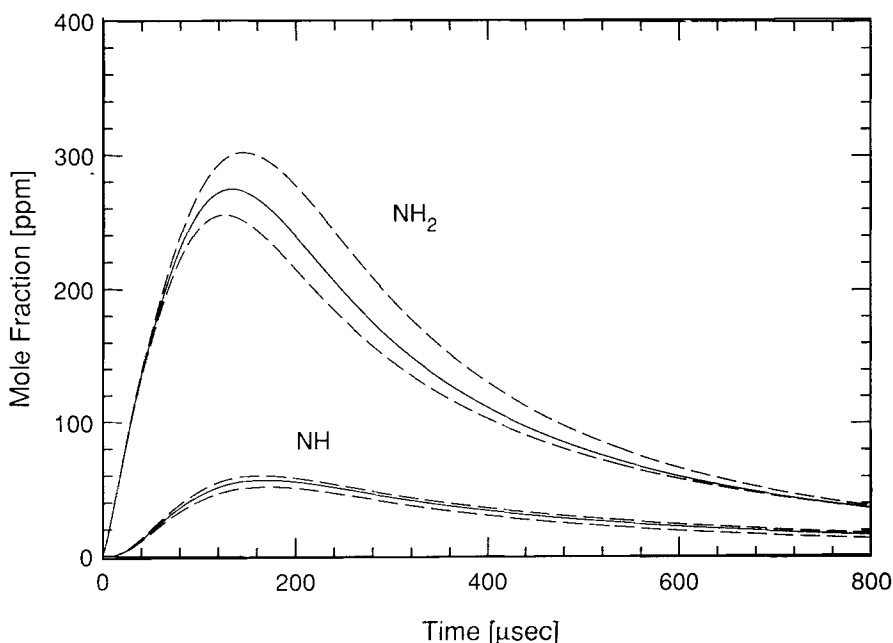
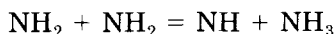


Figure 14. Influence of varying reaction (9) in the kinetic model. Solid line: rate coefficient found in Table I and dashed lines: $\pm 50\%$ variation. Model conditions as in Figure 7.

$10^{14}T^{-0.5}$. They expect a $T^{-0.5}$ temperature dependence for radical-radical reactions with no rearrangement. Miller use $k_{11} = 5 \times 10^{13}$ at 1200 K and they rank this reaction as important in the study of the oxidation of ammonia in flames [14]. Hanson and Salimian [18] give as an estimate 3.16×10^{13} in their study of NH_3 and NO. As well, they state that this reaction is part of a path that replenishes H and produces N_2 through a path not including NO. Dean, Chou, and Stern [21] give as a rate coefficient 5×10^{13} , while Cohen [17] gives as an estimate 3.16×10^{13} , Dransfeld [23] have measured this rate coefficient at room temperature as $8(\pm 3) \times 10^{13}$. They discuss the four possible product routes and give a preference to this channel at lower temperatures.

The fitting procedure for this reaction is similar to that of reaction (9). The best fit to our database is $k_{11} = 1.5 \times 10^{15}T^{-0.5}$ ($\pm 50\%$). At 2500 K, $k_{11} = 3.0 \times 10^{13}$. Examples of the variation of this rate coefficient on the modelled calculations for concentration are shown in Figure 15. The recent determinations of the other dominant NH loss paths reaction (-5) [9], $\text{H} + \text{NH} = \text{N} + \text{H}_2$, and reaction (7) [30], $\text{NH} + \text{NH} = \text{N}_2 + \text{H} + \text{H}$, allows us to reduce our uncertainty in this loss path. The use of the $T^{-0.5}$ temperature dependence and the room temperature rate coefficient of Dransfeld gives good agreement with our fitted rate coefficient as well as the intermediate temperature regime rate coefficient used by Miller.



The contribution factors shown in Figure 8 indicate that this reaction significantly influences the rise time of the NH data. Without a large con-

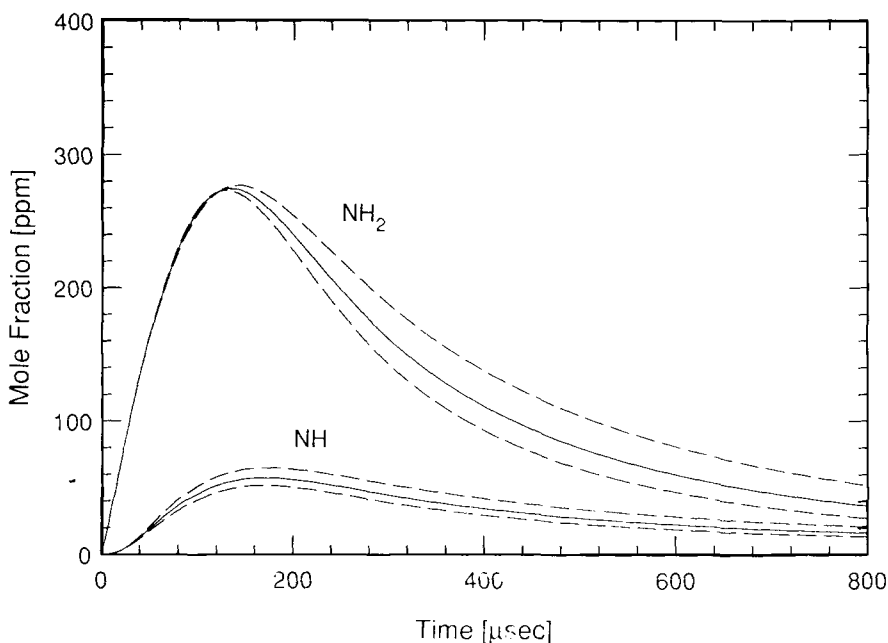


Figure 15. Influence of varying reaction (11) in the kinetic model. Solid line: rate coefficient found in Table I and dashed lines: $\pm 50\%$ variation. Model conditions as in Figure 7.

tribution by this reaction to the NH profiles, the model predictions of concentrations at early times would fall well below the experimental results.

It is not possible to explain the required rate of NH formation through the use of a large value of k_8 ($\text{NH}_2 + \text{M} \rightarrow \text{NH} + \text{H} + \text{M}$) and maintain the correct shape of the NH profile. A 10 fold increase in k_8 gives no improvement in fitting the rise time in the low temperature NH data and produces an anomalous peak shape to the concentration profile. It is also not possible to explain this early time behavior using an enlarged value of the rate coefficient of reaction (1a), $\text{NH}_3 + \text{M} \rightarrow \text{NH} + \text{H}_2$.

Various workers estimate values for k_{12} which range over an order of magnitude. Cohen [17] suggests $10^8 T^{1.5}$ and states that this route is likely to be important and can be estimated by comparison with the OH disproportionation rate. An extrapolation of his rate coefficient to room temperature is much higher than that given by Dransfeld [23] (less than 2×10^9). Miller [12] uses $5 \times 10^{12} \exp(-10000/RT)$ and Roose [1] uses $6.3 \times 10^{12} \exp(-10000/RT)$. Both are in agreement with Dransfeld. Bahn [35] gives $2 \times 10^{11} T^{0.623} \exp(-1810/RT)$ in agreement with Cohen.

The best fit to our database is given by $k_{12} = 5 \times 10^{13} \exp(-10000/RT)$ ($\pm 50\%$). At NH_3 pyrolysis temperatures, the temperature dependence of Miller and Roose ($E_A = 10000 \text{ cal mol}^{-1}$) is similar to that given by Cohen [17], yet allows for a rate coefficient that agrees with the room temperature value of Dransfeld. This present determination supports the suggestion by Cohen and Bahn of a large high temperature value of k_{12} . Examples showing the effect of the variation of this rate coefficient on the modelled profiles of NH and NH_2 are shown in Figure 16.

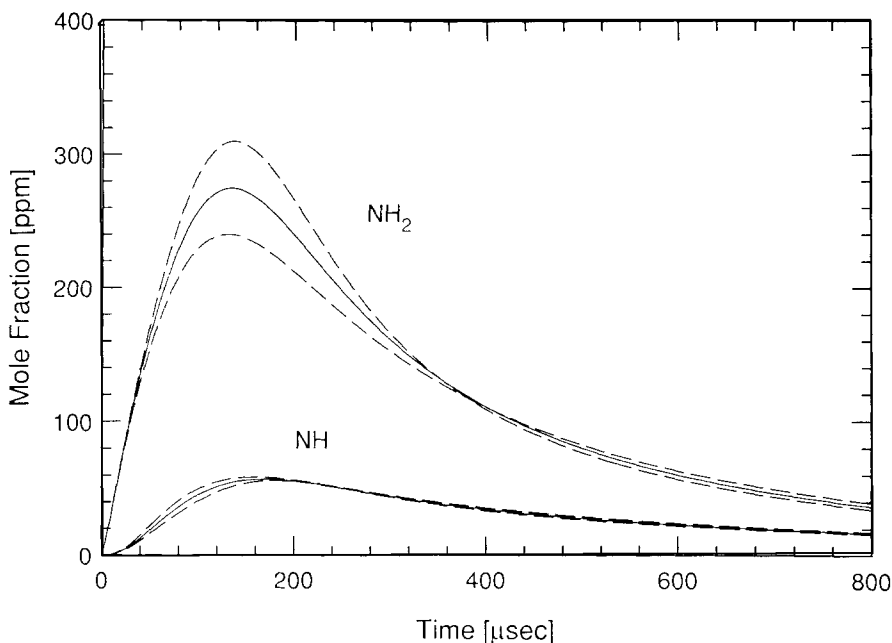


Figure 16. Influence of varying reaction (12) in the kinetic model. Solid line: rate coefficient found in Table I and dashed lines: $\pm 50\%$ variation. Model conditions as in Figure 7.

We were unable to infer the magnitude of any other product channels of the reaction, $\text{NH}_2 + \text{NH}_2 \rightarrow \text{products}$. Representative estimates of the rate coefficients of the various branch channels are shown in the Arrhenius diagram in Figure 17. The branch reactions which form product species with N—N bonds ($\text{N}_2\text{H}_2 + \text{H}_2$, $\text{N}_2\text{H}_3 + \text{H}$, and N_2H_4) are generally predicted to be much slower than reaction (12). As well, these branch reactions only slightly affect the H-atom and the NH profiles in our mechanism. Estimates of the rate coefficients for the branches which form N_2H_4 or $\text{N}_2\text{H}_3 + \text{H}$ are given by Dean [21]. Inclusion of a submechanism in the modelling which included these branch reactions did not significantly affect the fitted values of the rate coefficients of Reactions (9), (11), and (12).

Conclusion

An improved mechanism for the pyrolysis of NH_3 has been developed. It successfully predicts the measured concentrations of NH and NH_2 radicals over a wide range of reflected shock temperatures and NH_3 initial concentrations.

A database of experimental risetime and peak concentrations of NH and NH_2 is given for these pyrolysis conditions.

Constraints on the rate coefficients for the reactions $\text{NH}_2 + \text{H} \rightarrow \text{NH} + \text{H}_2$, $\text{NH}_2 + \text{NH} \rightarrow \text{N}_2\text{H}_2 + \text{H}$, and $\text{NH}_2 + \text{NH}_2 \rightarrow \text{NH} + \text{NH}_3$ have been derived from the NH and NH_2 profiles. An improved value for the rate coefficient of $\text{NH}_3 + \text{M} \rightarrow \text{NH}_2 + \text{H} + \text{M}$ is given based on the recent accurate measurement of $\text{NH}_3 + \text{H} \rightarrow \text{NH}_2 + \text{H} + \text{M}$.

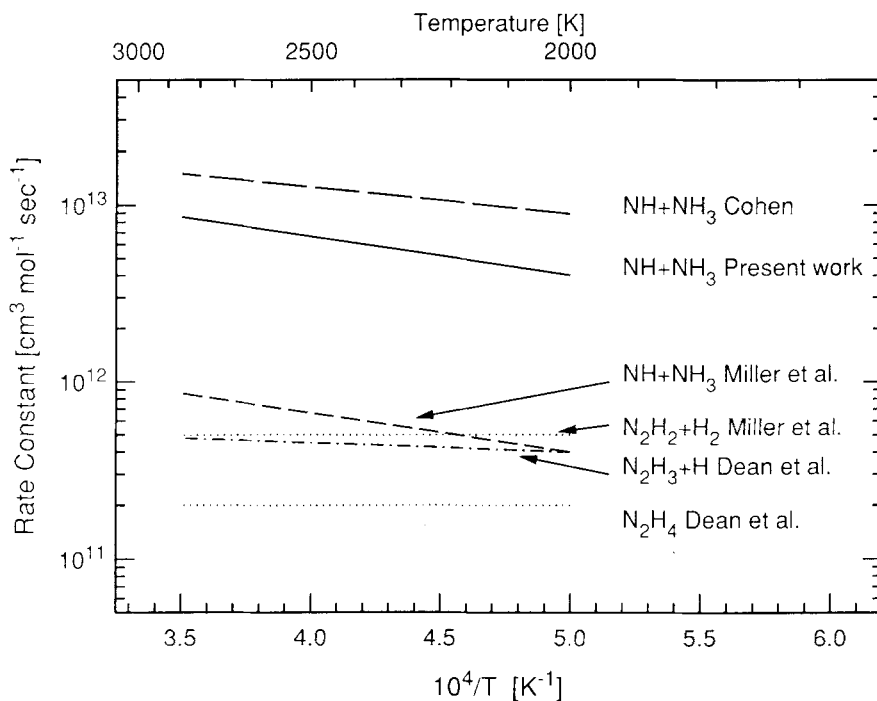


Figure 17. Arrhenius plot for the reaction: $\text{NH}_2 + \text{NH}_2 \rightarrow \text{Products}$. Solid line: branching product $\text{NH} + \text{NH}_3$, from the present work; long-dashed line: branching product $\text{NH} + \text{NH}_3$, from Cohen [17]; dashed line: branching product $\text{NH} + \text{NH}_3$, from Miller [12]; dot-dashed line: branching product $\text{N}_2\text{H}_3 + \text{H}$, from Dean [21]; lower dotted line: branching product N_2H_4 , Dean [21]; and upper dotted line: branching product $\text{N}_2\text{H}_2 + \text{H}_2$, from Miller [12].

Acknowledgment

This work has been supported by the Air Force Office of Scientific Research, Aerospace Sciences Directorate. One of us (KKH) was supported by the German Aerospace Research Establishment (DFVLR).

APPENDIX: Kinetic rates

Included in this listing are the majority of reactions considered in the combustion literature for ammonia pyrolysis. All rate coefficients are given in $\text{cm}^3 \text{mol}^{-1} \text{s}^{-1}$ with the activation energies in cal mol^{-1} .

(2) $\text{NH}_3 + \text{H} = \text{NH}_2 + \text{H}_2$. This rate coefficient is now well established at temperatures below 1800 K. A fit to a TST formulation of this rate coefficient to 2500 K accurate to $\pm 10\%$ has been given by Marshall and Fontijn [7] as $6.26 \times 10^2 T^{3.275} \exp(-8520/RT)$. Michael, Sutherland, and Klemm [5] give a value for the temperature range of 900 to 1777 K of $1.82 \times 10^{14} \exp(-16030/RT)$ accurate to $\pm 10\%$. They also give a three parameter fit to all their experimental data as $6.38 \times 10^5 T^{2.39} \exp(-10170/RT)$. This compares well to their theoretical formulation of $6.99 \times 10^6 T^{2.17} \exp(-12450/RT)$.

We use their three parameter experimental fit. (2(a)) $\text{NH}_3 + \text{NH} = \text{Products}$. This reaction has not been mentioned in the combustion literature other than in the form of reaction (12).

(3) $\text{H}_2 + \text{M} = \text{H} + \text{H} + \text{M}$ ($\text{M} = \text{Ar}$). In this study, the rate coefficient affects only the H atom profile at long times. The value given by Baulch [38] has been used. (3(a)) $\text{N}_2 + \text{M} = \text{N} + \text{N} + \text{M}$. This reaction is insignificant when argon is used as the carrier gas.

(4) $\text{NH} + \text{M} = \text{N} + \text{H} + \text{M}$ ($\text{M} = \text{Ar}$). Mertens [6] recently determined this rate coefficient from HNC0 shock tube experiments and gave a value of $2.65 \times 10^{14} \exp(-75500/RT)$ at high temperatures.

(5) $\text{NH} + \text{H} = \text{N} + \text{H}_2$. A recent determination of the reverse reaction rate coefficient in this laboratory gave $k_5 = 1.60 \times 10^{14} \exp(-25140/RT)$ [30]. The equivalent forward rate coefficient, k_5 , is also given as $3.2 \times 10^{13} \exp(-325/RT)$. This is in good agreement with the inference for k_5 by Morley [38] of 3×10^{13} .

(6) $\text{NH} + \text{N} = \text{H} + \text{N}_2$. The measured profiles of this present work are not sensitive to this rate. Miller [12] estimates a rate coefficient for this reaction of 3×10^{13} . An estimate quoted by Dean [21] of $6.3 \times 10^{11} T^{0.5}$ is equivalent over our present temperature range.

(7) $\text{NH} + \text{NH} = \text{N}_2 + \text{H} + \text{H}$. The rate coefficient for this reaction has recently been measured by Mertens [9] in a study of NHCO kinetics in a shock tube. They gave a value of 5.1×10^{13} independent of temperature over the range 2070 to 2730 K. The products given here are in agreement with Kajimoto [39] and Miller [12]. Dean [21] use a value of 5×10^{13} in their rich ammonia flames. (7(a)) $\text{NH} + \text{NH} = \text{N}_2 + \text{H}_2$. Cohen [17] gives a value of $1 \times 10^8 T^1$ for this reaction and states that this reaction and reaction (7(c)) are expected to be slower than reaction 10(b)). (7(b)) $\text{NH} + \text{NH} = \text{NNH} + \text{H}$. Hanson and Salimian [34] use an estimate of $7.94 \times 10^{11} T^{0.5} \exp(-10000/RT)$. This reaction has the same effect on their kinetics as reaction (7). Cohen gives a value for the rate coefficient of $10^9 T^{1.5}$ and a discussion of the temperature dependence of reactions (7(a)), (7(b)), and (7(c)). (7(c)) $\text{NH} + \text{NH} = \text{NH}_2 + \text{N}$. Hanson and Salimian give an estimate for this rate, $2 \times 10^{11} T^{0.5} \exp(-2000/RT)$ that indicates that it is probably not significant in the modelling of NH and NH_2 profiles compared to reaction (7).

(8) $\text{NH}_2 + \text{M} = \text{NH} + \text{H} + \text{M}$. This reaction does not have a significant effect on the measured concentration profiles of this work. The rate coefficient used is that of Hanson and Salimian [34]. Miller [12] uses a rate coefficient of $2 \times 10^{16} T^{-0.50}$ for the reverse reaction. This is an order of magnitude less at 2500 K than the estimate of Hanson and Salimian. (8(a)) $\text{NH}_2 + \text{M} = \text{N} + \text{H}_2 + \text{M}$. This is an unlikely product route that has not been considered in the combustion literature.

(10) $\text{NH}_2 + \text{N} = \text{N}_2 + \text{H} + \text{H}$. Whyte and Philips [40] have measured this rate coefficient at room temperature and give a rate coefficient of 7.3×10^{13} . This rate coefficient is used by Miller [12] as well. (10(a)) $\text{NH}_2 + \text{N} = \text{NNH} + \text{H}$. This reaction should be kinetically indistinguishable from reaction (10). Cohen [17] gives a rate coefficient value of 10^{14} . (10(b)) $\text{NH}_2 + \text{N} = \text{NH} + \text{NH}$. This branching path is mentioned only by Roose [1].

(13) $\text{NH}_2 + \text{NH}_2 = \text{N}_2\text{H}_2 + \text{H}_2$. All the product branches of these reactants may play some minor role in the NH_2 profiles under the present experimental conditions. It is not possible at present to place any strong limits on these reactions by kinetic fitting of the present data. A value of 5×10^{11} given by Khe is quoted by Miller [12], Roose [1], as well as Hanson and Salimian [34], gives a value of $4 \times 10^{13} \exp(-1200/RT)$. (13(a)) $\text{NH}_2 + \text{NH}_2 = \text{N}_2\text{H}_3 + \text{H}$. Dean [21] give a theoretical estimate of $7.4 \times 10^{11} \exp(-2490/RT)$ in good agreement with their flame data. They find it necessary to invoke this reaction to improve their modelling fits. (13(b)) $\text{NH}_2 + \text{NH}_2 = \text{N}_2\text{H}_4$. Dean gives a value of 2×10^{11} and a theoretical discussion. (13(c)) $\text{NH}_2 + \text{NH}_2 = \text{N}_2 + \text{H}_2 + \text{H}_2$. This rate coefficient is only described by Dove and Nip [2].

(14) $\text{NNH} + \text{M} = \text{N}_2 + \text{H} + \text{M}$. The measured profiles of this present work are not sensitive to this rate coefficient. Miller [12] has recently used a rate coefficient of $2 \times 10^{14} \exp(-20000/RT)$. This estimate has been derived from fits to flame measurements and a sensitivity to N_2 yields at temperatures near 1200 K. Dean, Hardy, and Lyon [41] give a rate coefficient of $1.5 \times 10^{15} \exp(-35000/RT)$ which they derived from their flame data at 1750 K. (14(a)) $\text{NNH} + \text{M} = \text{N} + \text{NH} + \text{M}$. This is an unlikely product route, mentioned only in the review by Hanson and Salimian [34].

(15) $\text{NNH} + \text{H} = \text{N}_2 + \text{H}_2$. The measured profiles of this present work are not sensitive to the value of rate. Hanson and Salimian [34] give a value of $4 \times 10^{13} \exp(-2980/RT)$ and Glarborg [16] use a similar rate. Miller and Bowman [12] have recently used a value of 1×10^{14} . (15(a)) $\text{NNH} + \text{N} = \text{N}_2 + \text{NH}$. This reaction is mentioned only in the review of Hanson and Salimian.

(16) $\text{NNH} + \text{NH} = \text{N}_2 + \text{NH}_2$. This rate coefficient does not have a significant effect on the measured profiles. Miller and Bowman [12] use a rate coefficient of 5×10^{13} . Hanson and Salimian [34] give a rate coefficient value of $2 \times 10^{11} T^{0.5} \exp(-2000/RT)$, a lower estimate.

(17) $\text{NNH} + \text{NH}_2 = \text{N}_2 + \text{NH}_3$. Miller [12] gives an estimate for this rate coefficient of 5×10^{13} . Dean [21] gives an estimate of 10^{13} .

(18) $\text{N}_2\text{H}_2 + \text{M} = \text{NNH} + \text{H} + \text{M}$. Miller [12-14] notes that the diimide reactions are not well established in the literature, and gives an estimate of the rate coefficient for this reaction of $5 \times 10^{16} \exp(-50000/RT)$. The present work is not sensitive to the value of this rate coefficient though this reaction contributes to the H concentration profile slightly. Dean, Chou, and Stern [21] use $3.4 \times 10^{12} \exp(-65000/RT)$ for the unimolecular decomposition of this reaction and give a brief theoretical discussion of this rate. (18(a)) $\text{N}_2\text{H}_2 + \text{M} = \text{N}_2 + \text{H}_2 + \text{M}$. This path is mentioned by Hanson and Salimian [34] only.

(19) $\text{N}_2\text{H}_2 + \text{H} = \text{NNH} + \text{H}_2$. Miller [12] uses a value of $5 \times 10^{13} \exp(-1000/RT)$ as an estimate for the rate coefficient. Dean, Chou, and Stern [21], in effective agreement with Miller, give $10^{12} T^{0.5} \exp(-2000/RT)$.

(20) $\text{N}_2\text{H}_2 + \text{NH} = \text{NNH} + \text{NH}_2$. Hanson and Salimian [34] gives an estimate for this rate coefficient of $10^{13} \exp(-1000/RT)$ as does Miller [12].

(21) $\text{N}_2\text{H}_2 + \text{NH}_2 = \text{NH}_3 + \text{NNH}$. Miller [12] and Hanson and Salimian [34] use $10^{13} \exp(-3980/RT)$ as an estimate. (21(a)) $\text{N}_2\text{H}_2 + \text{NH}_2 = \text{NH} + \text{N}_2\text{H}_3$. Only Hanson and Salimian mention this reaction path.

Various other reactions are mentioned in the literature but have no noticeable effect on our kinetic modelling.

$\text{NNH} + \text{NNH} = \text{N}_2\text{H}_2 + \text{N}_2$. This reaction is only mentioned by Hanson and Salimian [34]. $\text{NH}_3 + \text{NH}_2 = \text{N}_2\text{H}_3 + \text{H}_2$. Dove and Nip [2] give a value of $7.94 \times 10^{11} T^{0.5} \exp(-21560/RT)$ and this value is used by Roose, Hanson, and Salimian, and Yumura and Asaba. $\text{N}_2\text{H}_2 + \text{N}_2\text{H}_2 = \text{NNH} + \text{N}_2\text{H}_3$. This reaction is only mentioned by Hanson and Salimian [34]. Discussion of the role of N_2H_3 can be found in Dean [21], Miller [12], and Cohen [17].

Bibliography

- [1] T.R. Roose, Ph.D. Thesis, Stanford University, 1981.
- [2] E. J. Dove and W.S. Nip, *Can. J. Chem.*, **57**, 689 (1979).
- [3] K. Holzrichter and H. Gg. Wagner, *18th Symp. (Int.) on Combustion*, The Combustion Institute, Pittsburgh, 1981.
- [4] M. Yumura and T. Asaba, *18th Symp. (Int.) on Combustion*, The Combustion Institute, Pittsburgh, 1981.
- [5] J. V. Michael, J. W. Sutherland, and R. B. Klemm, *Int. J. Chem. Kinetics*, **17**, 315 (1985).
- [6] J. W. Sutherland and J. V. Michael, *J. Chem. Phys.*, **88**, 830 (1988).
- [7] P. Marshall and A. Fontijn, *J. Chem. Phys.*, **85**, 2637 (1986).
- [8] A. Y. Chang and R. K. Hanson, *J. Quant. Spectro. Radiat. Transfer*, **42**, 207 (1989).
- [9] J. D. Mertens, A. Y. Chang, R. K. Hanson, and C. T. Bowman, *Int. J. Chem. Kinet.*, **21**, 1049 (1989).
- [10] K. Kohse-Höinghaus, D. F. Davidson, and R. K. Hanson, *J. Quant. Spectrosc. Radiat. Transfer*, **42**, 1 (1989).
- [11] D. F. Davidson, A. Y. Chang, K. Kohse-Höinghaus, and R. K. Hanson, *J. Quant. Spectrosc. Radiat. Transfer*, **42**, 267 (1989).
- [12] J. A. Miller and C. T. Bowman, *Progress Energy Combust. Sci.*, in press (1988).
- [13] J. A. Miller, M. C. Branch, and R. J. Kee, *Comb. and Flame*, **43**, 81 (1981).
- [14] M. C. Branch, R. J. Kee, and J. A. Miller, *Comb. Sci. and Tech.*, **29**, 147 (1982).
- [15] J. A. Miller, M. D. Smooke, R. M. Green, and R. J. Kee, *Comb. Sci. and Tech.*, **34**, 149 (1983).
- [16] P. Glarborg, J. A. Miller, and R. J. Kee, *Comb. and Flame*, **65**, 177 (1986).
- [17] N. Cohen, *Int. J. Chem. Kinet.*, **19**, 319 (1987).
- [18] S. Salimian, R. K. Hanson, and C. H. Kruger, *Comb. and Flame*, **56**, 83 (1984).
- [19] S. Salimian, R. K. Hanson, and C. H. Kruger, *Int. J. Chem. Kinet.*, **16**, 725 (1984).
- [20] T. R. Roose, R. K. Hanson, and C. H. Kruger, *11th Intl. Symposium on Shock Tubes and Waves*, University Washington, 245 (1977).
- [21] A. M. Dean, M.-S. Chou, and D. Stern, *Int. J. Chem. Kinet.*, **16**, 633 (1984).
- [22] C. J. Dasch and R. J. Blint, *Comb. Sci. and Tech.*, **41**, 223 (1984).
- [23] P. Dransfeld, W. Hack, H. Kurzke, F. Temps, and H. Gg. Wagner, *20th Symp. (Int.) on Combustion*, The Combustion Institute, Pittsburgh, 1984.
- [24] M. Yumura, T. Asaba, Y. Matsumoto, and H. Matsui, *Int. J. Chem. Kinet.*, **12**, 439 (1980).
- [25] N. Fujii, H. Miyama, M. Koshi, and T. Asaba, *18th Symp. (Int.) on Combustion*, The Combustion Institute, Pittsburgh, 1981.
- [26] M. Yumura and T. Asaba, *14th Intl. Symposium on Shock Tube and Waves*, Sydney, 1983.
- [27] W. R. Anderson, *J. Phys. Chem.*, **93**, 530 (1989).
- [28] A. Y. Chang, E. Rea, Jr., and R. K. Hanson, *Appl. Optics*, **26**, 885 (1987).
- [29] N. L. Garland and E. R. Crosley, *J. Chem. Phys.*, **90**, 3566 (1989).
- [30] D. F. Davidson and R. K. Hanson, *Int. J. Chem. Kinet.*, in press, 1990.
- [31] R. J. Kee, J. A. Miller, and T. H. Jefferson, *CHEMKIN; A General Purpose Problem Independent Transportable Fortran Chemical Kinetics Code Package*, Sandia National Lab. Report No. SAND80-8003, 1980.
- [32] A. E. Lutz, R. J. Kee, and J. A. Miller, *SENKIN; A Fortran Program for Predicting Homogeneous Gas Phase Chemical Kinetics with Sensitivity Analysis*, Sand 87-8248, Sandia Nat. Lab., Livermore, 1988.

- [33] R. J. Kee, F. M. Rupley, and J. A. Miller, *The CHEMKIN Thermodynamic Database*, Sandia Nat. Lab. Report No. SAND87-8215, 1987.
- [34] R. K. Hanson and S. Salimian, *Combustion Chemistry*, W. C. Gardiner, Ed., Springer-Verlag, New York, 1985, Chap. 6.
- [35] G. S. Bahn, *Reaction Rate Compilation for H-O-N System*, Gordon and Breach, 1968.
- [36] S. W. Mayer, L. Schieler, and H. S. Johnston, *J. Chem. Phys.*, **45**, 385 (1966).
- [37] S. W. Mayer and L. Schieler, *J. Phys. Chem.*, **72**, 236 (1968).
- [38] C. Morley, *18th Symp. (Int.) on Combustion*, The Combustion Institute, Pittsburgh, 1981.
- [39] O. Kajimoto, T. Yamamoto, and T. Fueno, *J. Phys. Chem.*, **83**, 429 (1979).
- [40] A. R. Whyte and L. F. Phillips, *J. Phys. Chem.*, **88**, 5670 (1984).
- [41] A. M. Dean, J. E. Hardy, and R. K. Lyon, *19th Symp. (Int.) on Combustion*, The Combustion Institute, Pittsburgh, 1982.
- [42] S. C. Ross, F. W. Birss, M. Verloet, and D. A. Ramsay, *J. Mol. Spectro.*, **129**, 436 (1988).

Received July 12, 1989

Accepted December 6, 1989